ELSEVIER

Journal of Organometallic Chemistry 548 (1997) 211–221

Journal of Organometallic Chemistry

Diphenylborylated derivatives of organocobaloximes and organorhodoximes: synthesis, spectroscopic and structural characterisation

Fioretta Asaro, Renata Dreos *, Silvano Geremia, Giorgio Nardin, Giorgio Pellizer, Lucio Randaccio [1], Giovanni Tauzher, Sara Vuano

Dipartimento di Scienze Chimiche, Università di Trieste, 34127 Trieste, Italy

Received 13 May 1997

Abstract

A series of organometallic complexes derived by organocobaloximes and organorhodoximes in which either one or both the hydrogen bridges have been replaced by BPh_2 groups, $RM(DH)(DBPh_2)$*N*-MeIm and $RM((DBPh_2)_2$*N*-MeIm, respectively, have been synthesised and characterised, both in solution and in solid state. ^1H NMR spectra show that they assume different interconverting conformations in solution. With increasing steric bulk of R, the axial phenyls of the BPh_2 group tend to face *N*-MeIm, forcing the latter in an orientation which is quite unusual in organocobaloximes and causing a lengthening of the Co–N bond. Some possible implications on the strength of the *trans* Co–C bond are discussed. © 1997 Elsevier Science S.A.

Keywords: Organocobaloximes; Organorhodoximes; Boron substituted; Conformational equilibria; X-ray structures

1. Introduction

The organocobaloximes, $RCo(DH)_2L$, where R = alkyl group, DH = monoanion of dimethylglyoxime and L = neutral ligand, were synthesised at the beginning of the 1960s [1], and immediately became the subject of extensive studies, because they were considered good models of vitamin B_{12}. The large number of available derivatives with different R and L groups allowed systematic studies of the dependence of the molecular geometry and the solution behaviour on the steric and electronic properties of the axial ligands [2], and gave some basic information useful for the understanding of the more complex cobalamine system. The analogous rhodium derivatives, organorhodoximes, provided an insight into the effect of increasing the size of the metal centre [3–6]. Less information is available about the effects of modifications of the equatorial ligand, although systems with modified oxime bridges, such as the Costa et al.'s models [7] and the Lariat type complexes [8,9] are well known.

The metal complexes of the bis(dimethylglyoximato) ligand in which either one or both the hydrogen bridges have been replaced by BPh_2 groups are very interesting because they may assume different fast interconverting conformations in solution, depending on the interactions between the phenyls of the BPh_2 group and the axial ligands (Schemes 1 and 2).

The extensive work on the $Fe(DBPh_2)_2LL'$ complexes [10–15] showed that the π–π interactions play a crucial role in determining the conformations adopted

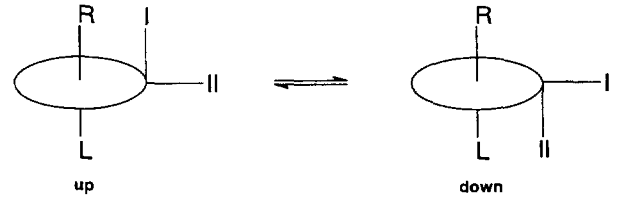

Scheme 1.

* Corresponding author. Università degli Studi di Trieste, Dipartimento di Scienze Chimiche, Via Licio Giorgieri 1, I-34127 Trieste. Fax: +39-40-676-3903.

[1] Also corresponding author.

PII S0022-328X(97)00405-1

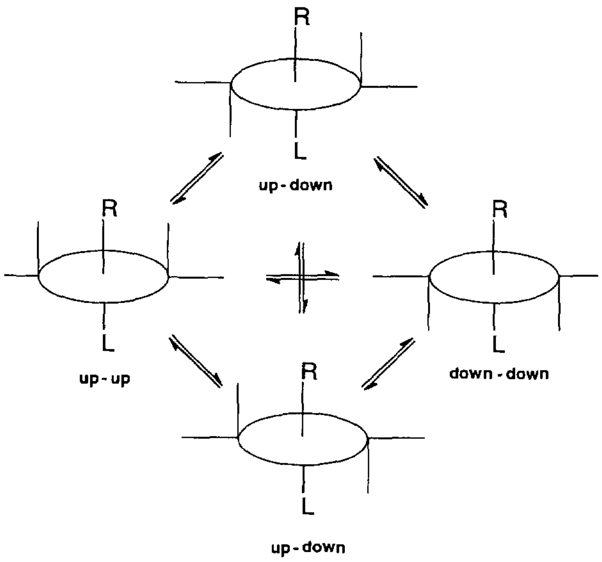

Scheme 2.

by these complexes. Our previous work [16–18] pointed out that the $\pi-\pi$ interactions may be the factor determining the adopted conformations in the diphenylborylated organocobaloximes and organorhodoximes too, at least when the steric bulk difference between the axial ligands is relatively small. A better understanding of the importance of the latter effect on the averaged conformation may be obtained from the examination of a series of derivatives containing R groups with systematically varying steric and electronic properties and the same neutral ligand L. It is interesting to note that when the complex assumes a conformation in which at least one phenyl of the BPh_2 group faces a planar neutral ligand L, the latter is forced in an orientation that bisects the five-membered rings of the equatorial moiety. This orientation is quite unusual in cobaloximes, while always occurs in (DO)(DOH)pn derivatives ((DO)(DOH)pn = $N^2,N^{2'}$-propane-1,3-diylbis(2,3-butanedione-2-imine-3-oxime)) and generally leads to a lengthening of the Co–N [19,20] and Co–C [20] bonds. Therefore, the insertion of one or two BPh_2 bridges in the bis(dimethylglyoximato) moiety may offer the opportunity of fine tuning the Co–C bond length through non bonded effects; this should affect its attitude towards the homolytic cleavage, which is currently accepted to be the first step of the reactions catalyzed by the vitamin B_{12} coenzyme [21–23].

2. Experimental section

Organocobaloximes [1], organorhodoximes [24–27], $MeCo(DH)(DBPh_2)$*N*-MeIm [16], $MeCo(DBPh_2)_2$*N*-MeIm [16], $MeRh(DH)(DBPh_2)$*N*-MeIm [17] and $MeCo(DBPh_2)_2$*N*-MeIm [17] have been synthesised as previously described. In order to obtain X-ray quality crystals, $CH_3Co(DBPh_2)_2$*N*-MeIm (**1**) was recrystallized from CH_2Cl_2/*i*-PrOH.

Solvent and reagents have been commercially purchased and were used without further purification.

^1H and ^{13}C spectra were recorded on a Jeol EX-400 (^1H at 400 MHz and ^{13}C at 100.4 MHz) from $CDCl_3$ solutions with TMS as internal standard.

2.1. Synthesis of the $RCo(DH)(DBPh_2)$N-MeIm derivatives

0.1 g of $RCo(DH)_2$*N*-MeIm were dissolved in about 50 ml of CH_2Cl_2 and an excess of diphenylborinic anhydride was added, the ratio [diphenylborinic anhydride]:[complex] being 2 for R = *n*-Pr and 4 for R = Ph. The solution was heated at 35°C for one day for R = *n*-Pr and for two days for R = Ph. Partial evaporation of the solvent afforded yellow powders, that were recrystallized from CH_2Cl_2/*i*-PrOH.

n-PrCo(DH)(DBPh$_2$)N-MeIm Anal. Found: C, 55.9; H, 6.3; N, 13.5. Calculated for $C_{27}H_{36}N_6O_4BCo$: C, 56.1; H, 6.3; N, 14.5%.

PhCo(DH)(DBPh$_2$)N-MeIm Anal. Found: C, 58.1; H, 5.6; N, 13.4. Calculated for $C_{30}H_{34}N_6O_4BCo$: C, 58.8; H, 5.6; N, 13.7%.

2.2. Synthesis of the $RCo(DBPh_2)_2$N-MeIm derivatives

0.1 g of $RCo(DH)_2$*N*-MeIm were dissolved in about 50 ml of CH_2Cl_2 with a five fold excess of diphenylborinic anhydride. Some drops of *N*-MeIm were added in order to avoid the dissociation of the axial base. The solutions were heated for one day for the alkyl derivatives and for four days for the phenyl derivative. The compounds were recrystallized from CH_2Cl_2/*i*-PrOH.

EtCo(DBPh$_2$)$_2$N-MeIm Anal. Found: C, 61.4; H, 6.0; N, 11.1. Calculated for $C_{38}H_{43}N_6O_4B_2Co$: C, 62.7; H, 5.9; N, 11.5%.

n-PrCo(DBPh$_2$)$_2$N-MeIm (**2**) Anal. Found: C, 59.0; H, 5.8; N, 10.1. Calculated for $C_{39}H_{45}N_6O_4B_2Co$: C, 58.1; H, 5.7; N, 10.2%.

n-BuCo(DBPh$_2$)$_2$N-MeIm Anal. Found: C, 62.9; H, 6.3; N, 10.6. Calculated for $C_{40}H_{47}N_6O_4B_2Co$: C, 63.5; H, 6.3; N, 11.1%.

PhCo(DBPh$_2$)$_2$N-MeIm Anal. Found: C, 64.3; H, 5.0; N, 10.1. Calculated for $C_{42}H_{43}N_6O_4B_2Co$: C, 65.0; H, 5.6; N, 10.8%.

2.3. Synthesis of the $RRh(DH)(DBPh_2)$N-MeIm derivatives

0.1 g of $RRh(DH)_2$*N*-MeIm were dissolved in about 50 ml of CH_2Cl_2 and an equimolar amount of diphenylborinic anhydride was added. The solution is allowed to stay at ambient temperature for two hours; partial evaporation of the solvent and the addition of few drops of *i*-propyl alcohol afforded yellow–brown crystals, that were recrystallized from CH_2Cl_2/MeOH.

EtRh(DH)(DBPh$_2$)N-MeIm Anal. Found: C, 50.4; H, 5.5; N, 13.7. Calculated for $C_{26}H_{34}N_6O_4BRh$: C, 51.3; H, 5.6; N, 13.8%.

n-PrRh(DH)(DBPh$_2$)N-MeIm Anal. Found: C, 50.2; H, 5.7; N, 13.2. Calculated for $C_{27}H_{36}N_6O_4BRh$: C, 52.1; H, 5.8; N, 13.5%.

i-PrRh(DH)(DBPh$_2$)N-MeIm Anal. Found C, 51.2; H, 5.9; N, 13.0. Calculated for $C_{27}H_{36}N_6O_4BRh$: C, 52.1; H, 5.8; N, 13.5%.

2.4. Synthesis of the RRh(DBPh$_2$)$_2$N-MeIm derivatives

To 0.1 g of RRh(DH)$_2$ *N*-MeIm dissolved in about 50 ml of CH_2Cl_2, a four fold amount of diphenylborinic anhydride was added. The solutions were refluxed for 6 h. The compounds were isolated by evaporation of the solvent.

EtRh(DBPh$_2$)$_2$N-MeIm Anal. Found C, 57.4; H, 5.5; N, 11.0. Calculated for $C_{38}H_{43}N_6O_4B_2Rh$: C, 59.1; H, 5.6; N, 10.9%.

n-PrRh(DBPh$_2$)$_2$N-MeIm Anal. Found: C, 56.9; H, 5.7; N, 10.5. Calculated for $C_{39}H_{45}N_6O_4B_2Rh$: C, 59.6; H, 5.8; N, 10.7%.

i-PrRh(DBPh$_2$)$_2$N-MeIm Anal. Found: C, 57.2; H, 5.6; N, 10.7. Calculated for $C_{39}H_{45}N_6O_4B_2Rh$: C, 59.6; H, 5.8; N, 10.7%

2.5. X-ray structure determinations

Crystal data for MeCo(DBPh$_2$)$_2$*N*-MeIm (**1**) and n-PrCo(DBPh$_2$)$_2$*N*-MeIm (**2**) are collected in Table 1. The diffraction data were collected on an Enraf–Nonius CAD4 diffractometer. Accurate unit cell parameters and orientation matrix were determined by least-squares refinement of the setting angles of 25 well-centered reflections in the range $20° < 2\theta < 28°$. Data were collected at room temperature in $\omega/2\theta$ scan mode. The intensities of three representative reflections were measured every 2 h of X-ray exposure time and no decay throughout the data collection was observed. Intensity data were corrected for Lorentz and polarization factors. No absorption correction was applied. The structures were solved by Patterson and Fourier methods and refined by least-squares method, treating anisotropically all the non-H species. H-atoms were placed at calculated positions, with isotropic temperature factors equal to those of the atoms to which they are bonded. Their contribution was held constant in the refinements. The choice of the centrosymmetric space group for **1** implied a statistical disorder of the axial ligand. Therefore the refinement of the structure was carried out also in the acentric *P*1 space group, but it resulted in a higher R value (0.071) and in significant differences in the chemically equivalent bond lengths. For **2** one disordered methylene chloride molecule per Co atom was detected on the Fourier maps. Furthermore, the *N*-methylimidazole ligand was found disordered with two

Table 1
Crystal data for **1** and **2**

Compound	**1**	**2**
Formula	$C_{37}H_{41}CoB_2N_6O_4$	$C_{40}H_{49}CoCl_2B_2N_6O_4$
M	714.33	829.34
a (Å)	8.276(2)	17.301(4)
b (Å)	10.512(3)	14.477(4)
c (Å)	11.479(3)	18.446(4)
α (deg)	68.23(2)	90
β (deg)	73.91(3)	117.32(5)
γ (deg)	73.34(3)	90
V (Å^3)	871.9(7)	4105(1)
Z	1	4
Crystal system	triclinic	monoclinic
Space group	$P\bar{1}$	$P2_1/n$
D_{calc}(g cm^{-3})	1.36	1.34
μ (Mo Kα)(cm^{-1})	5.4	5.9
F (000)	374	1736
Crystal size (mm^3)	0.3 × 0.3 × 0.6	0.2 × 0.4 × 0.7
2ϑ (Mo Kα) (deg)	56	56
No. measured reflections	4386	10578
No. independent reflections [$I > 3\sigma(I)$]	2212	3796
No. variables	259	541
Weight	$4F^2/[\sigma(I)+(0.04F)^2]$	$4F^2/[\sigma(I)+(0.04F)^2]$
$R(F_o)$	0.056	0.067
$R_w(F_o)$	0.061	0.069
Residuals in *F*-map (e Å^{-3})	0.85	0.95

Table 2
Positional Parameters of **1**, $MeCo(DBPh_2)_2$ *N*-MeIm

Atom	*x*	*y*	*z*	*B* (Å^2)
Co	0.000	0.000	0.000	3.16(2)
O1	0.1409(4)	0.0906(3)	−0.2669(3)	3.90(8)
O2	0.2900(4)	0.1310(3)	−0.1233(3)	3.90(8)
N1	0.0094(4)	0.0417(4)	−0.1730(3)	3.28(9)
N2	0.1784(5)	0.0821(4)	−0.0148(3)	3.57(9)
N3[a]	−0.179(1)	0.1785(8)	0.0174(7)	4.3(2)
N4[a]	−0.384(1)	0.3755(9)	−0.0373(9)	4.8(2)
C1	−0.0898(7)	−0.0003(6)	−0.3362(5)	5.1(1)
C2	−0.0926(6)	−0.0056(5)	−0.2057(4)	3.7(1)
C3	−0.2171(6)	−0.0732(5)	−0.0920(4)	3.9(1)
C4	−0.3613(7)	−0.1209(5)	−0.1019(5)	4.7(1)
C5	0.0819(7)	0.3359(5)	−0.2467(5)	4.4(1)
C6	0.0775(7)	0.4210(6)	−0.1766(5)	5.0(1)
C7	−0.0308(8)	0.5472(6)	−0.1840(6)	6.1(2)
C8	−0.140(1)	0.5974(7)	−0.2722(7)	7.9(2)
C9	−0.144(1)	0.5201(8)	−0.3405(7)	9.7(2)
C10	−0.0324(9)	0.3924(7)	−0.3310(6)	7.5(2)
C11	0.3821(7)	0.2170(5)	−0.3600(5)	4.5(1)
C12	0.4931(8)	0.2979(6)	−0.3664(6)	5.7(2)
C13	0.6246(8)	0.3307(7)	−0.4722(7)	6.9(2)
C14	0.6538(8)	0.2793(7)	−0.5705(6)	6.3(2)
C15	0.5544(9)	0.1971(8)	−0.5638(6)	7.0(2)
C16	0.4183(8)	0.1669(7)	−0.4616(5)	6.1(2)
C17[a]	0.184(1)	−0.175(1)	−0.0006(8)	3.3(2)
C18[a]	−0.237(2)	0.242(1)	0.1017(9)	5.2(3)
C19[a]	−0.357(1)	0.360(1)	0.074(1)	5.2(3)
C20[a]	0.484(2)	−0.504(2)	−0.108(1)	7.3(4)
C21[a]	−0.279(1)	0.269(1)	−0.0774(9)	4.6(3)
B1	0.2187(8)	0.1927(6)	−0.2458(5)	3.9(1)

[a]Occupancy factor = 0.5.

orientations differing by a rotation of 180° around the Co–N axial bond, with occupancy factors of 0.66 and 0.33. Refinement parameters are given in Table 1. Programs used for calculations were supplied as a package by Enraf–Nonius (Molen). Atomic scattering factors are taken from Ref. [28]. Final positional and thermal parameters are given in Tables 2 and 3. Tables of anisotropic thermal parameters, H-atom coordinates and a full list of bond lengths and angles have been deposited at the Cambridge Crystallographic Data Centre.

3. Results

3.1. Syntheses

The complexes containing BPh_2 bridges have been obtained by reacting the corresponding

Table 3
Positional Parameters of **2**, *n*-$PrCo(DBPh_2)_2$ *N*-MeIm

Atom	*x*	*y*	*z*	*B* (Å^2)
Co	0.01883(5)	0.01188(6)	0.25866(5)	2.80(2)
O1	0.0065(3)	0.2005(3)	0.2058(3)	3.6(1)
O2	−0.0640(3)	0.0817(3)	0.0953(3)	3.9(1)
O3	0.1112(3)	−0.0576(3)	0.4214(2)	3.2(1)
O4	0.0264(3)	−0.1749(3)	0.3109(2)	3.3(1)
N1	0.0351(3)	0.1398(4)	0.2688(3)	2.9(1)
N2	−0.0497(3)	0.0076(4)	0.1458(3)	3.5(1)
N3	0.0951(3)	0.0158(4)	0.3700(3)	3.0(1)
N4	0.0058(3)	−0.1163(4)	0.2477(3)	3.0(1)
C1	0.1240(5)	0.2664(5)	0.3550(4)	4.4(2)
C2	0.0923(4)	0.1697(5)	0.3401(4)	3.2(2)
C3	0.1236(4)	0.0970(5)	0.4002(4)	3.3(2)
C4	0.1806(5)	0.1131(6)	0.4896(4)	4.8(2)
C5	−0.0826(6)	0.2504(7)	0.0616(5)	4.1(2)
C6	−0.0732(6)	0.3450(7)	0.0846(6)	5.2(3)
C7	−0.0836(7)	0.4136(8)	0.0251(7)	6.3(3)
C8	−0.1052(7)	0.3880(9)	−0.0543(7)	6.4(3)
C9	−0.1135(8)	0.2953(9)	−0.0767(7)	7.1(4)
C10	−0.1023(7)	0.2276(8)	−0.0176(6)	5.7(3)
C11	−0.1607(6)	0.1746(7)	0.1418(5)	4.1(2)
C12	−0.1675(7)	0.2307(9)	0.1996(7)	5.9(3)
C13	−0.2448(7)	0.237(1)	0.2066(7)	7.4(4)
C14	−0.3176(7)	0.1878(9)	0.1543(7)	7.0(4)
C15	−0.3134(7)	0.130(1)	0.0963(8)	7.2(4)
C16	−0.2346(6)	0.1262(8)	0.0880(7)	5.5(3)
C17	−0.1138(6)	−0.0891(6)	0.0228(5)	5.3(2)
C18	−0.0711(5)	−0.0730(5)	0.1137(4)	4.0(2)
C19	−0.0434(4)	−0.1464(5)	0.1742(4)	3.8(2)
C20	−0.0708(6)	−0.2440(6)	0.1553(5)	5.6(2)
C21	0.1054(5)	−0.2209(6)	0.4554(5)	3.5(2)
C22	0.0333(6)	−0.2153(8)	0.4716(5)	4.7(3)
C23	0.0284(7)	−0.2716(9)	0.5328(6)	6.1(3)
C24	0.0945(8)	−0.3327(9)	0.5765(7)	6.9(4)
C25	0.1643(8)	−0.3406(9)	0.5602(7)	7.0(4)
C26	0.1713(7)	−0.2836(8)	0.5005(6)	5.5(3)
C27	0.1937(5)	−0.1722(6)	0.3740(5)	3.3(2)
C28	0.2742(6)	−0.1305(8)	0.4248(6)	4.9(3)
C29	0.3499(6)	−0.1544(8)	0.4189(7)	5.6(3)
C30	0.3461(7)	−0.2194(8)	0.3602(6)	5.5(3)
C31	0.2659(6)	−0.2610(8)	0.3102(6)	5.4(3)
C32	0.1910(6)	−0.2378(6)	0.3173(5)	4.1(2)
B1	−0.0759(5)	0.1741(5)	0.1279(5)	3.3(2)
B2	0.1104(5)	−0.1547(5)	0.3897(4)	3.3(2)
C33	0.1243(4)	0.0125(5)	0.2345(4)	3.9(2)
C34	0.1308(5)	−0.0453(6)	0.1752(5)	6.0(2)
C35	0.2218(5)	−0.0375(7)	0.1806(5)	7.1(2)
N5	−0.0823(3)	0.0124(4)	0.2886(3)	4.2(1)
N6[a]	−0.1622(7)	0.0456(9)	0.3508(9)	13.8(4)
C36	−0.0900(6)	0.0609(8)	0.3430(7)	11.7(3)
C37[a]	−0.221(1)	0.097(1)	0.3652(9)	9.7(5)
C38[a]	−0.2004(7)	−0.007(2)	0.3027(8)	12.8(7)
C39	−0.1508(6)	−0.036(1)	0.2588(7)	12.3(4)
N61[b]	−0.208	−0.015	0.295	10
C381[b]	−0.175	0.045	0.336	8
C371[b]	−0.296(2)	−0.007(2)	0.279(2)	9(1)
Cl1[c]	0.4586(6)	0.0282(6)	0.2603(5)	10.4(3)
Cl2[c]	0.4794(6)	0.0110(8)	0.1148(6)	12.2(3)
Cl3[d]	0.553(1)	0.012(1)	0.219(1)	13.0(6)
Cl4[d]	0.391(1)	−0.005(1)	0.0879(9)	12.2(6)
Cl5[e]	−0.482(2)	0.022(2)	0.257(2)	19(1)
Cl6[e]	−0.613(2)	0.027(2)	0.140(2)	14.8(9)
C40	0.451(2)	0.073(1)	0.168(1)	18(1)

Notes to Table 3:
[a]Occupancy factor = 0.667; [b]Occupancy factor = 0.333; [c]Occupancy factor = 0.5; [d]Occupancy factor = 0.3; [e]Occupancy factor = 0.2.

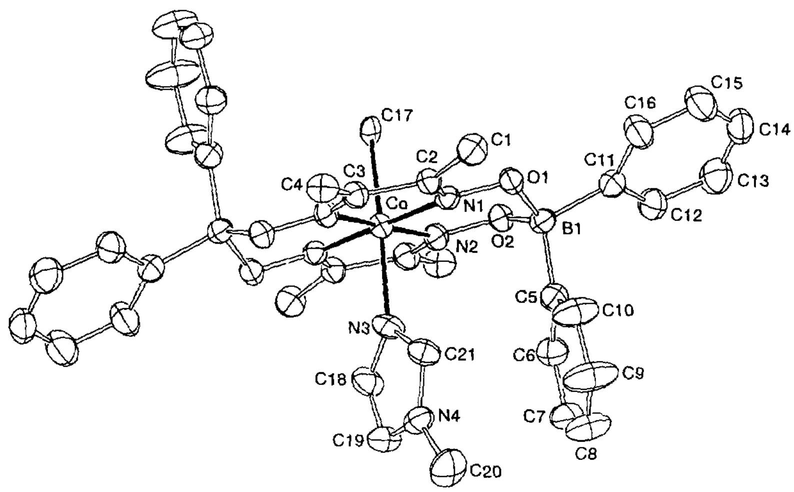

Fig. 1. ORTEP drawing of **1** together with the atom numbering scheme.

organocobaloximes and organorhodoximes with diphenylborinic anhydride.

As previously outlined for the methyl derivative [16–18] the resulting products can contain either one or two boron bridges, depending on the ratio [diphenylborinic anhydride]:[complex]. Starting from $MeCo(DH_2)_2$*N*-MeIm the monoborylated complex has been obtained using a ratio less than one and the diborylated complex using an excess of anhydride [16]; $MeRh(DBPh_2)_2$*N*-MeIm is less stable than the corresponding Co derivative and loses easily one boron bridge in solution [17].

For bulkier R groups the insertion of the BPh_2 groups becomes more difficult, specially for Rh complexes, so that larger amounts of anhydride and longer reaction times are required. Borylated derivatives of Co complexes containing bulky R groups, as *i*-Pr, could not be isolated because they decompose, owing to the lability of the Co–C bond.

The diborylated Rh complexes were isolated in the presence of an excess of anhydride, but they lose easily a BPh_2 group in solution, so that could not be recrystallized.

3.2. Structural results

The ORTEP drawing of **1** is shown in Fig. 1, together with the atom numbering scheme. Owing to the location of the molecule of **1** on a crystallographic symmetry centre, the axial ligands are superimposed. However, the least-square refinement allows to distin-

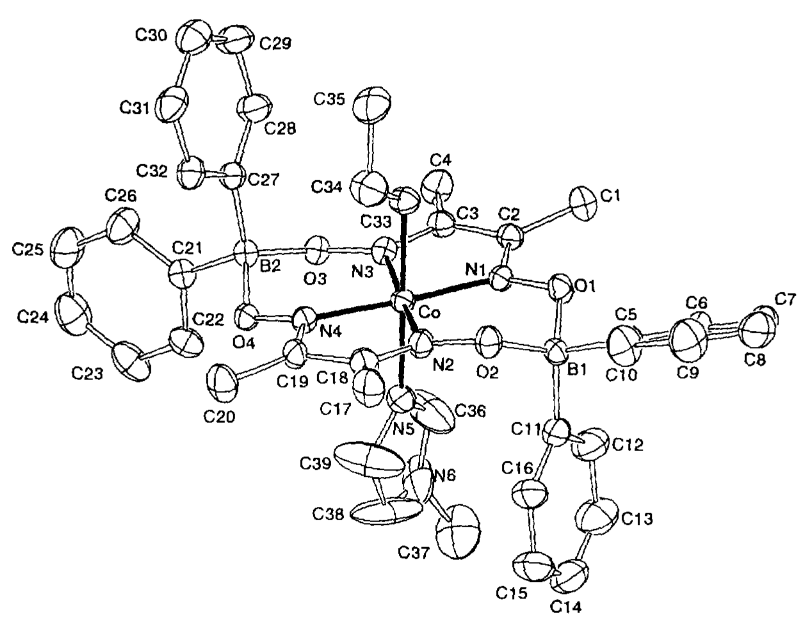

Fig. 2. ORTEP drawing of **2** together with the atom numbering scheme.

guish the two axial donor atoms. For sake of clarity, only one of the two orientations is shown in Fig. 1, where the 'up–down' conformation of the axial phenyl groups is highlighted. Thus, one phenyl group faces the *N*-MeIm ligand, the other, the axial methyl group. Such a conformation of the equatorial ligand is similar to that reported for the analogous complex $MeCo(DBPh_2)_2MeOH$ [16]. The mean equatorial Co–N distance is 1.853(5) Å, very close to the value of 1.863(5) Å reported for the MeOH derivative. The C–Co–N axial fragment has Co–C and Co–N distances of 2.021(8) Å and 2.068(7) Å, respectively, which do not differ significantly from those of 2.009(7) Å and 2.058(5) Å reported for the corresponding cobaloxime $MeCo(DH)_2$*N*-MeIm [29]. The Co–C and Co–N distances in the monoborylated complex $MeCo(DH)(DBPh_2)$*N*-MeIm are 2.00(1) Å and 2.014(9) Å, respectively. The Co–N axial bond shorter than in the diborylated analogue corresponds to a different orientation of *N*-MeIm with respect to the equatorial ligand. The O...O distance of 2.523(6) Å does not differ significantly from that already reported for $MeCo(DBPh_2)_2MeOH$ [16] of 2.519(6) Å. These figures are significantly larger than those, averaging to 2.487(2) Å, between the oxygens bound by a hydrogen bond in cobaloximes [30].

The ORTEP drawing of **2** is shown in Fig. 2, together with the atom numbering scheme. The crystal is built up by molecules of **2** and crystallization CH_2Cl_2 molecules in a ratio 1:1. The latter molecules have three different orientations with approximate occupancies of 0.5, 0.3 and 0.2, respectively, due to the different positioning of Cl atoms bound to the central C atom. The *N*-MeIm ligand has two orientations differing by a rotation of 180° about the Co–N5 bond. As in **1**, the equatorial ligand has an 'up–down' conformation, one axial phenyl group facing the *N*-MeIm ligand, the other the axial propyl ligand. The mean plane of each axial phenyl ring is approximately parallel to the plane of the axial ligand to which it is faced. The mean Co–N equatorial distance of 1.867(5) Å is that expected for these complexes (see above). The C–Co–N axial fragment is characterised by Co–C and Co–N bond lengths of 2.068(8) Å and 2.063(7) Å, respectively. Comparison with the corresponding figures in **1** shows that there is a significant lengthening of the Co–C bond in **2**, due to the bulk and to the σ-donor power of the *n*-Pr ligand larger than those of the Me one [31]. The O...O mean distance of 2.527(6) Å is very close to that found in **1**.

3.3. NMR Results

3.3.1. Bis(dimethylglyoximato) moiety

The Co and the Rh derivatives show similar changes of the ^{13}C and ^{1}H chemical shifts of the bis(dimethylglyoximato) frame after the insertion of the BPh_2 groups (Tables 4 and 5). In the monoborylated complexes, the CN and CH_3 carbons and CH_3 protons on the boron bridge side are less shielded than in the corresponding cobaloximes or rhodoximes, whereas those on the hydrogen bridge side resonate close to the latter. In the diborylated complexes the equatorial CN and CH_3 carbons and the CH_3 protons are deshielded with respect to the corresponding parent cobaloximes and rho-

Table 4
^{13}C and ^{1}H NMR data of the dimethylglyoximate moiety in $[RCo(DH)_{2-n}(DBPh_2)_n$*N*-MeIm] complexes[a]

R	*n*	CN		CH_3		CH_3	
		DH	$DBPh_2$	DH	$DBPh_2$	DH	$DBPh_2$
Me[b]	0	–	–	–	–	2.13	–
	1	147.6	154.9	12.0	13.0	2.15	2.39
	2	–	154.2	–	13.2	–	2.45
Et	0	–	–	–	–	2.13	–
	1	–	–	–	–	2.20	2.42
	2	–	153.9	–	13.2	–	2.49
n-Pr	0	–	–	–	–	2.13	–
	1	147.6	154.7	12.0	13.1	2.18	2.41
	2	–	153.9	–	13.2	–	2.47
n-Bu	0	–	–	–	–	2.12	–
	1	–	–	–	–	2.18	2.41
	2	–	–	–	–	–	2.47
Ph	0	–	–	–	–	2.04	–
	1	148.5	156.1	12.3	13.3	2.19	2.37
	2	–	154.7	–	13.4	–	2.44

[a] δ in ppm from TMS, $CDCl_3$ solutions.
[b] Ref. [16].

Table 5
^{13}C and ^{1}H NMR data of the bisdimethylglyoximate moiety in $[RRh(DH)_{2-n}(DBPh_2)_n$*N*-MeIm] complexes[a]

R	*n*	CN		CH_3		CH_3	
		DH	$DBPh_2$	DH	$DBPh_2$	DH	$DBPh_2$
Me[b]	0	148.6	–	11.8	–	2.14	–
	1	148.2	153.7	11.9	12.9	2.19	2.40
	2	–	153.1	–	12.9	–	2.43
Et	0	–	–	–	–	2.15	–
	1	148.0	153.5	11.8	12.9	2.22	2.43
	2	–	152.7	–	12.9	–	2.45
n-Pr	0	–	–	–	–	2.16	–
	1	148.1	153.6	11.9	13.0	2.22	2.43
	2	–	152.8	–	12.9	–	2.43
i-Pr	0	148.7	–	11.8	–	2.14	–
	1	148.0	153.6	11.9	13.0	2.26	2.46
	2	–	152.6	–	–	–	2.50

[a] δ in ppm from TMS, $CDCl_3$ solutions.
[b] Ref. [17].

doximes and resonate close to those on the boron side of the monoborylated derivatives.

3.3.2. Axial ligands

3.3.2.1. Co derivatives. The introduction of the first diphenylborinic group increases the shielding of all the *N*-methylimidazole protons in the order Me < *n*-Pr ≈ *n*-Bu < Et < Ph, the magnitude of the effect being different at various protons. In the diborylated derivatives the *N*-MeIm protons are further shielded. For all these complexes, except for the phenyl derivative, the insertion of the second bridge causes a larger effect than that of the first (Table 6).

The protons of the axial alkyls also are shielded upon introduction of the first diphenylborinic group. The magnitude of the effect decreases in the order Me > *n*-Pr ≈ *n*-Bu > Et for the protons at α carbon and is almost constant for those at β and γ carbons. Noticeably, the effect becomes larger on going from α to β to γ position. The phenyl bonded to Co is the only axial ligand in the RCo(DH)($DBPh_2$)*N*-MeIm series showing its whole proton spectrum shifted to higher frequencies with respect to the parent RCo$(DH)_2$*N*-MeIm complex.

In the diborylated derivatives the protons at the α carbon of the axial alkyls are less shielded than in the monoborylated ones, whereas those at the β and γ carbons are shielded, the shielding effect being smaller for the former. The protons of the phenyl bonded to the metal are less shielded in the diborylated than in the monoborylated derivative.

Table 6
^{1}H NMR data of the axial ligands in [RCo$(DH)_{2-n}(DBPh_2)_n$*N*-MeIm] complexes[a]

R	*n*	*N*-MeIm H-2	H-4	H-5	CH_3	R Hα	Hβ	Hγ	Hδ
Me[b]	0	7.44	6.94	6.78	3.66	0.72	–	–	–
	1	7.44	7.02	6.71	3.58	0.16	–	–	–
	2	6.06	6.40	6.45	3.27	0.39	–	–	–
Et	0	7.42	6.95	6.76	3.62	1.62	0.37	–	–
	1	6.83	6.68	6.56	3.43	1.37	0.01	–	–
	2	5.78	5.98	6.00	3.13	1.66	−0.07	–	–
n-Pr	0	7.42	6.95	6.76	3.62	1.52	0.94	0.78	–
	1	6.99	6.75	6.60	3.46	1.22	0.57	0.40	–
	2	5.97	6.15	6.18	3.19	1.49	0.47	0.23	–
n-Bu	0	7.42	6.94	6.75	3.62	1.52	0.87	1.18	0.78
	1	6.99	6.76	6.59	3.46	1.21	0.51	0.75	0.62
	2	5.97	6.15	6.18	3.19	1.53	0.39	0.58	0.62
Ph	0	7.57	7.08	6.79	3.66	7.39	6.94–6.89 (m+p)	–	–
	1	5.88	6.01	6.30	3.25	7.53	6.95–6.85 (m+p)	–	–
	2	5.47	5.34	5.33	2.94	7.71	7.00–6.90 (m+p)	–	–
free		7.41	7.05	6.86	3.67	–	–	–	–

[a] δ in ppm from TMS, $CDCl_3$ solutions.
[b] Ref. [16].

Table 7
^{1}H NMR data of the axial ligands in [RRh$(DH)_{2-n}(DBPh_2)_n$*N*-MeIm] complexes[a]

R	*n*	*N*-MeIm H-2	H-4	H-5	CH_3	R Hα	Hβ	Hγ
Me[b]	0	7.35	6.84	6.76	3.61	0.19	–	–
	1	6.89	6.75	6.63	3.50	−0.34	–	–
	2	5.69	6.45	6.40	3.26	−0.40	–	–
Et	0	7.33	6.82	6.76	3.61	1.14	0.60	–
	1	6.20	6.44	6.48	3.37	0.90	0.42	–
	2	5.56	5.97	6.04	3.15	0.83	0.18	–
n-Pr	0	7.31	6.82	6.75	3.61	–	0.76	–
	1	6.31	6.47	6.50	3.35	0.85–0.75	–	0.57
	2	5.68	6.14	6.16	3.20	0.65–0.57	–	0.32
i-Pr	0	7.29	6.80	6.73	3.60	1.30	0.76	–
	1	5.69	6.11	6.33	3.26	1.37	0.76	–
	2	5.35	5.41	5.56	3.00	1.50	0.68	–

[a] δ in ppm from TMS, $CDCl_3$ solutions.
[b] Ref. [17].

3.3.2.2. Rh derivatives. For the rhodoximes the insertion of the first BPh_2 bridge increases the shielding of the *N*-methylimidazole protons in the order Me < *n*-Pr < Et < *i*-Pr. The second borylation causes a further shielding, but, differently from the corresponding Co complexes, smaller than the first (Table 7).

The protons of the axial R groups are shielded upon introduction of the first diphenylborinic group for R = Me, Et and *n*-Pr, like for the Co analogues. For R = *i*-Pr, the proton at the α carbon is deshielded and those at the β carbon slightly shielded.

In the diborylated derivatives the protons at the α carbon show a further slight shielding for R = linear alkyl. The shielding effect is greater for the protons at the β and γ carbons and comparable with that caused by the first borylation. For R = *i*-Pr, the proton at the α carbon is less shielded than in the monoborylated derivative, whilst the protons at the β carbon are more shielded.

3.3.3. BPh_2 groups

Both in the monoborylated and in the diborylated series the phenyls of the BPh_2 groups show two sets of ^{13}C and of ^1H signals (Tables 8 and 9).

For PhCo(DH)($DBPh_2$)*N*-MeIm as well as for PhCo$(DBPh_2)_2$*N*-MeIm one set of proton signals shows the maximum deshielding and the other the maximum shielding. On going from the phenyl to the methyl derivative, the signals tend to merge. A similar trend is

Table 8
^1H and ^{13}C NMR data of BPh_2 groups in $[RCo(DH)_{2-n}(DBPh_2)_n N\text{-MeIm}]$ complexes[a]

R	n	^1H			^{13}C		
		ortho	*meta*	*para*	*ortho*	*meta*	*para*
Me[b]	1	7.61	7.23	7.14	131.7	127.1	125.7
		7.29	7.16	7.06	131.5	127.1	125.1
	2	7.33	7.16	7.13	131.8	127.1	125.7
		7.25	7.03	obs	131.8	126.7	125.5
Et	1	–	–	–			
	2	7.40	7.17	7.10			
		7.10	6.90	obs			
n-Pr	1	7.43	7.17	7.12			
		7.39	7.10	7.06			
	2	7.35	7.17	7.10			
		7.11	6.96	6.96			
n-Bu	1	–	–	–			
	2	7.34	7.16	7.10			
		7.10	6.96	6.96			
Ph	1	7.64	7.28	7.19			
		7.00	6.87	6.99			
	2	7.52	7.24	7.18			
		6.87	6.76	6.76			

[a] δ in ppm from TMS, $CDCl_3$ solutions.
[b] Ref. [16].

observed on going from the *i*-propyl to the methyl in the monoborylated rhodium derivatives.

The spectra of the diborylated rhodoximes were run in the presence of an excess of diphenylborinic anhydride owing to the tendency of these complexes to dissociate a diphenylboryl group in solution; consequently the proton resonances of the BPh_2 bridges are partially hidden.

Table 9
^1H and ^{13}C NMR data of BPh_2 groups in $[RRh(DH)_{2-n}(DBPh_2)_n N\text{-MeIm}]$ complexes[a]

R	n	^1H			^{13}C		
		ortho	*meta*	*para*	*ortho*	*meta*	*para*
Me[b]	1	7.50	7.18	7.08	131.9	127.0	125.5
		7.36	7.15	7.02–7.11	131.9	126.9	125.4
	2	7.32	7.18	7.02–7.11	132.2	127.0	125.8
		7.25	7.04	obs	132.2	126.8	125.6
Et	1	7.47	7.20	7.11	132.0	126.6	125.0
		7.28	7.00	obs	132.0	126.9	125.7
	2	obs	obs	obs	132.2	126.9	125.9
		obs	obs	obs	131.9	126.4	125.0
n-Pr	1	7.46	7.19	7.13	132.0	127.0	125.7
		7.31	7.03	7.01	131.9	126.7	125.1
	2	7.39	7.19	7.14	132.2	127.0	125.9
		7.14	6.96	6.96	132.0	126.5	125.2
i-Pr	1	7.54	7.21	7.13	132.2	126.9	125.9
		7.35	6.87	7.07	132.0	126.3	124.5
	2	obs	obs	obs	132.2	126.9	125.9
		obs	obs	obs	132.1	126.0	124.3

[a] δ in ppm from TMS, $CDCl_3$ solutions.
[b] Ref. [17].

4. Discussion

4.1. Solution studies

Fruitful conformational investigations of diphenylborylated Fe(II)bis(dimethylglyoximates) [10–15], methylcobaloximes [16] and methylrhodoximes [17] through ^1H NMR were possible, since the magnetic anisotropy of the phenyls of the BPh_2 group causes a remarkable upfield shift of the proton resonances of the axial ligands facing them. The electronic effect of the borylation should cause deshielding [16,17], but this effect decays with the increasing number of interposed bonds and does not affect protons three or more bonds apart from the metal centre. Thus, the increase of the shielding effect ($\delta RCo(DH)(DBPh_2)N\text{-MeIm} - \delta RCo(DH)_2 N\text{-MeIm}$) for the *N*-MeIm protons and its concomitant decrease for those at the α carbon of the R group on going from R = Me to R = Ph in $RCo(DH)(DBPh_2)N$-MeIm (Table 6) indicate that the ratio 'down'/'up' increases in the order Me < *n*-Pr ≈ *n*-Bu < Et < Ph, the methyl derivative being almost in the 'up' form and the phenyl derivative almost in the 'down' form (Scheme 1). The same trend is observed in the $RRh(DH)(DBPh_2)N$-MeIm derivatives on going from R = Me to R = *i*-Pr (Table 7); the population of conformer 'down' is higher than in the corresponding Co derivatives for R = Me [17], Et, *n*-Pr and the population of conformer 'up' is not negligible for R = *i*-Pr.

Inspection of the signals of the BPh_2 protons (Tables 8 and 9) supports these conclusions. In $PhCo(DH)(DBPh_2)N$-MeIm the two sets of the BPh_2 protons resonances are well separated, showing one the maximum deshielding and the other one the maximum shielding. This is in accordance with the compound being almost always in the 'down' form, with phenyl II shielded because of the anisotropy of the *N*-MeIm facing it and phenyl I equatorial and deshielded (Scheme 1). In the methyl derivative, where the conformer 'up' is strongly predominant, one group of protons resonates at about the same frequencies than those of I in $PhCo(DH)(DBPh_2)N$-MeIm and are assigned to phenyl II, which is most of the time equatorial; [2] the other group of signals, more shielded, are assigned to phenyl

[2] It should be noted that the equatorial positions are not strictly equivalent in the conformers 'up' and 'down'.

I, mostly axial facing Me. Therefore, for the BPh_2 protons, the shielding increases in the order equatorial < axial facing alkyl < axial facing *N*-MeIm. As phenyl II exchanges between a deshielded equatorial and a strongly shielded axial position and phenyl I exchanges between a moderately shielded axial and a deshielded equatorial position, the shift of the conformational equilibrium from 'down' to 'up' leads to a shielding of phenyl I and to a deshielding of phenyl II and to the intermingling of the two sets of resonances. The same trend is observed in the Rh derivatives on going from the *i*-propyl to the methyl derivative.

For the diborylated complexes the change in proton shielding of the axial ligands on going from Me to Ph for $RCo(DBPh_2)_2$*N*-MeIm and from Me to *i*-Pr for $RRh(DBPh_2)_2$*N*-MeIm reflects an increasing population of conformer 'down–down' and a decreasing population of conformer 'up–up'. The electronic effect of the second BPh_2 group causes a deshielding of the α carbons of R. Indeed this effect, present in all the conformers, prevails on the ring current shielding, effective only in some of them. The electronic effect has a smaller influence on the protons at β and γ carbons, which are shielded. The deshielding of the protons of the Co bound phenyl in $PhCo(DBPh_2)_2$*N*-MeIm and that of the CH proton in *i*-$PrRh(DBPh_2)_2$*N*-MeIm reflects the small population of 'up–up' and 'up–down' conformers and the noticeable electron-withdrawing effect of the BPh_2 group.

The trend of the shifts of the BPh_2 protons on going from Ph- to Me-$Co(DBPh_2)_2$*N*-MeIm is similar to that present in the monoborylated derivatives, well in line with the above conclusions. For the phenyl derivative, where the conformation 'down–down' prevails, the two groups of resonances are well separated. As the conformational equilibrium moves from right to left (Scheme 2) the signals tend to intermingle and become very close for the methyl derivative.

The shielding effect on the CH_3 protons of *N*-MeIm offers an interesting insight into the influence of the R group on the conformational equilibrium. The insertion of the first boron bridge induces a shift variation of −0.41 ppm in the phenyl derivative, almost exclusively 'down' in solution. On going from the parent to the diborylated complexes the shift variation is very close to this value when R is a linear alkyl. (M = Co: −0.39 ppm for R = Me, −0.40 ppm for R = Et, −0.43 ppm for R = *n*-Pr and *n*-Bu; M = Rh: −0.35 ppm for R = Me, −0.46 ppm for R = Et, −0.41 ppm for R = *n*-Pr). These results indicate one phenyl facing the *N*-MeIm on average. For $PhCo(DBPh_2)_2$*N*-MeIm and *i*-$PrRh(DBPh_2)_2$*N*-MeIm the values are higher (−0.72 and −0.60 ppm, respectively) in agreement with a prevailing 'down–down conformation', especially for $PhCo(DBPh_2)_2$*N*-MeIm. The effectiveness of the phenyl group in forcing the monoborylated derivatives in the 'down' conformation and the diborylated derivatives in the 'down–down' conformation may be due to a cooperative effect between the π–π repulsive interactions of R with the side phenyls and the steric bulk of the R group. The latter should play a crucial role in determining the conformation of the *i*-propyl rhodium derivatives. Unexpectedly, the ethyl derivatives show a little but systematic deviation within the series of linear alkyls.

4.2. Structural results and possible implications as vitamin B_{12} models

The possibility of exploiting the steric and electronic properties of the R group to determine the conformations of these complexes offers an interesting chance of fine tuning the length of the axial bonds. Indeed, in the conformations where L faces at least one phenyl of the BPh_2 group, it is constrained in the orientation *B* (Fig. 3), bisecting the five-membered rings of the equatorial moiety. This orientation is quite rare in cobaloximes. In fact, in more than fifty cobaloximes, the L ligand assumes the orientation *A* with respect to the equatorial moiety [30], as shown in Fig. 3a for $MeCo(DH)_2Im$ (Im = imidazole), where the Co–Im distance is 2.019(3) Å [32]. The rare orientation *B* has been found only in two cobaloximes, $RCo(DH)_2$ *N*-MeIm with R = Me (Fig. 3b) and CH_2CH_2CN, the Co–*N*-MeIm distance being 2.058(5) Å in the methyl derivative [33]. In the analogous Costa et al. models the orientation *B* is always found, as in $\{MeCo[(DO)(DOH)pn](N\text{-MeIm})\}^+$, where the Co–*N*-MeIm distance is 2.042(2) Å [28] (Fig. 3c). On this basis, it was concluded that the Co–N axial bond is significantly longer in the orientation *B* than in the orientation *A* [19,20,30].

A similar correlation is observed in the borylated cobaloximes. Indeed, on going from $MeCo(DH)_2$*N*-MeIm, where *N*-MeIm has the orientation *B*, to $MeCo(DH)(DBPh_2)$*N*-MeIm, where *N*-MeIm has the orientation *A* (Fig. 3d), the Co–N bond becomes noticeably shorter. The insertion of the second BPh_2 bridge again leads to an orientation *B* of *N*-MeIm (Fig. 3e), which is forced to face the phenyl in the 'up–down' conformation and the Co–N bond lengthens. It is worthwhile to note that no difference in Rh–N axial distances is found when the corresponding $MeRh(DH)(DBPh_2)$*N*-MeIm and $MeRh(DH)_2$*N*-MeIm complexes are compared, since *N*-MeIm has the same orientation *B* in both complexes [17].

Comparison of the Co–Me distances (Fig. 3) seems to suggest that also the Co–C distance slightly increases on going from orientation *A* to orientation *B*. The difference is small, specially in view of the e.s.d.'s in borylated complexes, but could be significant and is in agreement with some recent findings. Indeed, the Co–C bonds in the $RCo(DH)_2Me_3Bzm$ (Me_3Bzm = 3,5,6

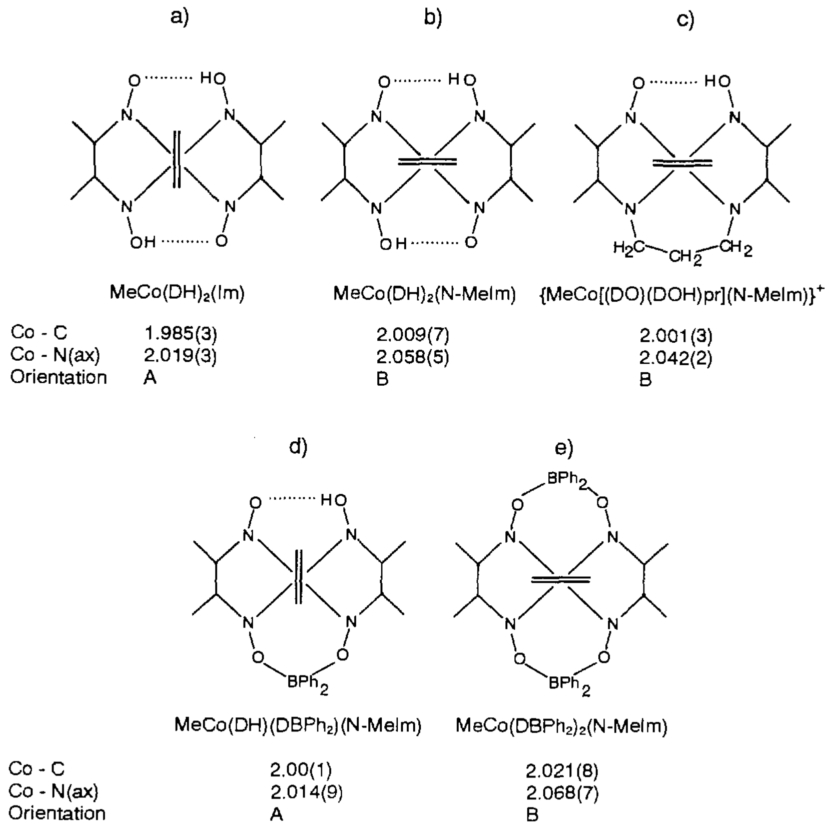

Fig. 3. Axial bonds lengths (Å) and orientation of the planar L ligand in methyl derivatives of some vitamin B_{12} models.

trimethylbenzimidazole) complexes, where the neutral ligand has essentially the orientation *A*, have been found to be slightly shorter (0.01–0.03 Å) than in the analogous $\{MeCo[(DO)(DOH)pn](Me_3Bzm)\}^+$ cations, where the neutral ligand adopts an orientation close to *B*, within ±30° [20]. Furthermore, in organocobaloximes and related models containing pyridine as neutral ligand, the ν_{Co-Me} stretching frequencies are slightly higher when py has the orientation *A* [34].

There is some evidence in cobaloximes of a correlation between the length of the axial Co–N bond [35] and the bond dissociation energy of the trans Co–C bond [36]. Furthermore, it has been suggested that the long Co–N (histidine) bond (2.5 Å) found in the methylmalonylCoA mutase [37] could be responsible for the activation (weakening) of the Co–adenosyl bond in the enzyme, facilitating the homolytic Co–C cleavage [38]. In borylated cobaloximes a weakening of the Co–C bond could be induced in the ground state by the orientation of the L ligand, which in turn is influenced by the interactions between L and the side phenyl groups. Therefore, the borylated cobaloximes seem to be a potentially interesting model for the vitamin B_{12} system.

Acknowledgements

We are grateful to CNR (Rome) and to Murst (Rome) for the financial support.

References

[1] G.N. Schrauzer, Inorganic Syntheses, in: R. Parry (Ed.) Vol. 11 (1968), p. 61.
[2] N. Bresciani-Pahor, M. Forcolin, L.G. Marzilli, L. Randaccio, M.F. Summers, P.J. Toscano, Coord. Chem. Rev. 63 (1985) 1, and references therein.
[3] N. Bresciani-Pahor, R. Dreos Garlatti, S. Geremia, L. Randaccio, G. Tauzher, E. Zangrando, Inorg. Chem. 29 (1990) 3437.
[4] L. Randaccio, S. Geremia, R. Dreos Garlatti, G. Tauzher, F. Asaro, G. Pellizer, Inorg. Chim. Acta 194 (1992) 1.
[5] S. Geremia, L. Randaccio, R. Dreos, G. Tauzher, Gazz. Chim. Ital. 125 (1995) 95.
[6] F. Asaro, G. Costa, R. Dreos, G. Pellizer, W. von Philipsborn, J. Organomet. Chem. 513 (1996) 193.
[7] G. Costa, G. Mestroni, E. De Savorgnani, Inorg. Chim. Acta 3 (1969) 323.
[8] L.G. Marzilli, A. Gerli, A.M. Calafat, Inorg. Chem. 31 (1992) 4617.
[9] A. Gerli, M. Sabat, L.G. Marzilli, J. Am. Chem. Soc. 114 (1992) 6711.

[10] M. Verhage, D.A. Hoogwater, H. van Bekkum, J. Reedijk, Recl. Trav. Chim. Pays Bas 101 (1982) 351.
[11] D.V. Stynes, D.B. Leznoff, D.G.A.H. de Silva, Inorg. Chem. 32 (1993) 3989.
[12] G. Impey, D.V. Stynes, J. Am. Chem. Soc. 115 (1993) 7868.
[13] D.V. Stynes, Inorg. Chem. 33 (1994) 5022.
[14] D.G.A.H. de Silva, D.B. Leznoff, G. Impey, I. Vernik, Z. Jin, D.V. Stynes, Inorg. Chem. 34 (1995) 4015.
[15] I. Vernik, D.V. Stynes, Inorg. Chem. 35 (1996) 6210.
[16] R. Dreos, G. Tauzher, S. Vuano, F. Asaro, G. Pellizer, G. Nardin, L. Randaccio, S. Geremia, J. Organomet. Chem. 505 (1995) 135.
[17] F. Asaro, R. Dreos, S. Geremia, G. Nardin, G. Pellizer, L. Randaccio, G. Tauzher, S. Vuano, J. Organomet. Chem. 525 (1996) 71.
[18] R. Dreos, S. Geremia, G. Nardin, L. Randaccio, G. Tauzher, Inorg. Chim. Acta, in press.
[19] N. Bresciani-Pahor, L. Randaccio, E. Zangrando, Inorg. Chim. Acta 168 (1990) 115.
[20] S.M. Polson, R. Cini, C. Pifferi, L.G. Marzilli, Inorg. Chem. 36 (1997) 314.
[21] D. Dolphin (Ed.), B_{12}, Wiley, New York, 1982.
[22] J.M. Pratt, Inorganic Chemistry of Vitamin B_{12}, Academic Press, London, 1972.
[23] J.M. Pratt, Chem. Soc. Rev. 63 (1985) 161, and references therein.
[24] J.H. Espenson, R.C. Mc Hatton, Inorg. Chem. 20 (1981) 3090.
[25] J.H. Weber, G.N. Schrauzer, J. Am. Chem. Soc. 92 (1970) 726.
[26] R. Dreos Garlatti, G. Tauzher, G. Costa, Inorg. Chim. Acta 121 (1986) 27.
[27] R. Dreos Garlatti, G. Tauzher, Polyhedron 9 (1990) 2047.
[28] International Tables for X-ray Crystallography; Kynoch Press: Birmingham, England, 1974, vol. IV.
[29] A. Bigotto, E. Zangrando, L. Randaccio, J. Chem. Soc. Dalton Trans., (1976) 96.
[30] L. Randaccio, N. Bresciani-Pahor, E. Zangrando, L.G. Marzilli, Chem. Soc. Rev. 18 (1989) 225.
[31] L. Randaccio, S. Geremia, E. Zangrando, C. Ebert, Inorg. Chem. 33 (1994) 4641.
[32] V. Pattabhi, M. Nethaji, E.J. Gabe, F.L. Lee, Y. La Page, Acta Cryst. C 40 (1984) 1115.
[33] A. Bigotto, E. Zangrando, L. Randaccio, J. Chem. Soc. Dalton Trans., (1976) 96.
[34] S. Hirota, S.M. Polson, J.M. Puckett Jr., S.J. Moore, M.B. Mitchell, L.G. Marzilli, Inorg. Chem. 35 (1996) 5646.
[35] M. Summers, P.J. Toscano, N. Bresciani-Pahor, G. Nardin, L. Randaccio, L.G. Marzilli, J. Am. Chem. Soc. 105 (1983) 6259.
[36] F.T.T. Ng, G.L. Rempel, C. Mancuso, J. Halpern, Organometallics 9 (1990) 2762.
[37] F. Mancia, N.H. Keep, A. Nagagawa, P.F. Leadley, S. Mc-Sweeney, B. Rasmussen, P. Boseke, O. Diat, R.P. Evans, Structure 4 (1996) 339.
[38] F.T.T. Ng, G. Rempel, J. Halpern, J. Am. Chem. Soc. 104 (1982) 621.